

OCT 13 1981

OCT 21 1981

AFWAL-TR-81-2020



## DETERMINATION OF AERODYNAMICALLY ADEQUATE FILLET GEOMETRY IN TURBOCOMPRESSOR BLADE ROWS

Lucien L. DeBruge

Technology Branch  
Turbine Engine Division

May 1981

TECHNICAL REPORT AFWAL-TR-81-2020

Final Report for Period April 1980 - February 1981

Property of U.S. Air Force  
AEDC LIBRARY  
FAC600-81-C-0034

Approved for public release; distribution unlimited.

AERO PROPULSION LABORATORY  
AIR FORCE WRIGHT AERONAUTICAL LABORATORIES  
AIR FORCE SYSTEMS COMMAND  
WRIGHT-PATTERSON AIR FORCE BASE, OHIO 45433

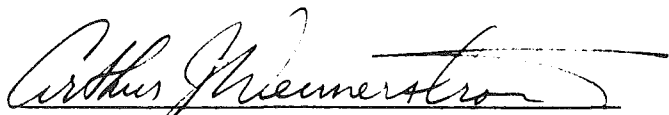
PROPERTY OF U.S. AIR FORCE  
AEDC TECHNICAL LIBRARY  
ARNOLD AFB, TN 37389

NOTICE

When Government drawings, specifications, or other data are used for any purpose other than in connection with a definitely related Government procurement operation, the United States Government thereby incurs no responsibility nor any obligation whatsoever; and the fact that the government may have formulated, furnished, or in any way supplied the said drawings, specifications, or other data, is not to be regarded by implication or otherwise as in any manner licensing the holder or any other person or corporation, or conveying any rights or permission to manufacture use, or sell any patented invention that may in any way be related thereto.

This report has been reviewed by the Office of Public Affairs (ASD/PA) and is releasable to the National Technical Information Service (NTIS). At NTIS, it will be available to the general public, including foreign nations.

This technical report has been reviewed and is approved for publication.

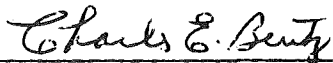


ARTHUR J. WENNERSTROM, GS-15  
Chief, Compressor Research Group



WALKER H. MITCHELL, GS-15  
Chief, Technology Branch

FOR THE COMMANDER



CHARLES H. BENTZ  
Acting Deputy Director  
Turbine Engine Division

"If your address has changed, if you wish to be removed from our mailing list, or if the addressee is no longer employed by your organization please notify AFWAL/POTX W-PAFB, OH 45433 to help us maintain a current mailing list".

Copies of this report should not be returned unless return is required by security considerations, contractual obligations, or notice on a specific document.

REPORT DOCUMENTATION PAGE		READ INSTRUCTIONS BEFORE COMPLETING FORM
1. REPORT NUMBER AFWAL-TR-81-2020	2. GOVT ACCESSION NO.	3. RECIPIENT'S CATALOG NUMBER
4. TITLE (and Subtitle) DETERMINATION OF AERODYNAMICALLY ADEQUATE FILLET GEOMETRY IN TURBOCOMPRESSOR BLADE ROWS		5. TYPE OF REPORT & PERIOD COVERED Final Report for Period April 1980 - February 1981
		6. PERFORMING ORG. REPORT NUMBER
7. AUTHOR(s) Lucien L. DeBruge		8. CONTRACT OR GRANT NUMBER(s)
9. PERFORMING ORGANIZATION NAME AND ADDRESS Aero Propulsion Laboratory (AFWAL/POTX) Air Force Wright Aeronautical Laboratories (AFSC) Wright-Patterson AFB, Ohio 45433		10. PROGRAM ELEMENT, PROJECT, TASK AREA & WORK UNIT NUMBERS Project: 2307 Task: S1 Work Unit: 27
11. CONTROLLING OFFICE NAME AND ADDRESS Aero Propulsion Laboratory (AFWAL/POTX) Air Force Wright Aeronautical Laboratories (AFSC) Wright-Patterson AFB, Ohio 45433		12. REPORT DATE May 1981
14. MONITORING AGENCY NAME & ADDRESS (if different from Controlling Office)		13. NUMBER OF PAGES 36
		15. SECURITY CLASS. (of this report) Unclassified
		15a. DECLASSIFICATION/DOWNGRADING SCHEDULE
16. DISTRIBUTION STATEMENT (of this Report) Approved for public release; distribution unlimited.		
17. DISTRIBUTION STATEMENT (of the abstract entered in Block 20, if different from Report)		
18. SUPPLEMENTARY NOTES		
19. KEY WORDS (Continue on reverse side if necessary and identify by block number)		
20. ABSTRACT (Continue on reverse side if necessary and identify by block number) A method for determining the fillet radius likely to prevent separation of the corner flow at the intersection of an airfoil and a hub or shroud where no relative motion or gap is present is described. A computer program was written which, from the physical dimensions of the blading and the flow characteristics at the blading entrance and exit, calculates the corner boundary layer parameters allowing the prediction of the required fillet radius. An incompressible turbulent flow, with the influence of endwall boundary layer secondary flow on the development of the corner boundary layer, is considered.		

FOREWORD

This report describes a method for determining the fillet radius likely to prevent separation of the corner flow at the intersection of an airfoil and a hub or shroud where no relative motion is present. The work was performed in the Turbine Engine Division of the Aero Propulsion Laboratory, Air Force Wright Aeronautical Laboratories, Wright-Patterson Air Force Base, Ohio. It was accomplished under Project 2307, Task S1, Work Unit 27. The effort was conducted by Dr. Lucien L. Debruge (AFAPL/POTX) during the period April 1980 to February 1981.

## TABLE OF CONTENTS

SECTION		PAGE
I	INTRODUCTION	1
II	THEORY AND METHODS	2
	1. Flow Model	2
	2. Calculation of Two-Dimensional Boundary Layer Momentum Thickness	4
	3. Calculation of Corner Flow Parameters	5
	4. Determination of Fillet Radius Likely to Prevent Corner Flow Separation	7
	5. Remarks Concerning the Calculation of $H_{12}$ , $\beta$ , and EU	7
III	NUMERICAL EXAMPLE	9
	1. Remarks	10
	APPENDIX: NUMERICAL METHODS (PROGRAM FILLET)	11
	1. Program Structure	11
	2. Program and Subprogram Descriptions	12
	3. FORTRAN Nomenclature	13
	4. Input Data	15
	5. Definition of Input Data Items	15
	6. Output Data	18
	7. Program Listing	19
	REFERENCES	36

## LIST OF ILLUSTRATIONS

FIGURE		PAGE
1	Non-Dimensional Velocity Along Mid-Channel and Pressure Corner Streamlines Assuming Circular Arc Blade	19
2	Non-Dimensional Velocity Along Mid-Channel and Pressure Corner Streamlines From Polynomial Interpolation of Data Points	20
3	Influence of Endwall Boundary Layer Secondary Flow on the Development of Corner Boundary Layer	21
4	Interference Displacement Thickness of Turbulent Boundary Layer in Convergent or Divergent Flow Along a Corner From (3)	22
5	Percentage Drop in Interference Displacement Thickness vs Fillet Radius	23
6	Variation of $H_{12}$ and $\delta/\epsilon_0$ Along the Pressure Corner	24
7	Non-Dimensional Velocity Profile Along Mid-Channel Streamline (WSXM) and Pressure Corner (WSX)	25
8	Non-Dimensional Velocity Profile Along Mid-Channel (WSXM) and Suction Corner (WSX) Streamlines	26
9	Average Euler Number Calculated Along Mid-Channel Streamline	27
10	Two-Dimensional (DEL2X) and Three-Dimensional (DEL2XS) Boundary Layer Momentum Thickness Along Pressure Corner	28
11	Two-Dimensional (DEL2X) and Three-Dimensional (DEL2XS) Boundary Layer Momentum Thickness Along Suction Corner	29
12	Variation of $\beta$ and $H_{12}$ Along Pressure Corner	30
13	Variation of $\beta$ and $H_{12}$ Along Suction Corner	31
14	Variation of Endwall Boundary Layer Thickness $\epsilon_0$ Along Pressure Corner	32
15	Variation of Endwall Boundary Layer Thickness $\epsilon_0$ Along Suction Corner	33

## LIST OF ILLUSTRATIONS (CONCLUDED)

FIGURE		PAGE
16	Variation of Corner Interference Displacement Thickness in Pressure Corner	34
17	Variation of Corner Interference Displacement Thickness in Suction Corner	35

## LIST OF SYMBOLS

$C_f$	Skin friction coefficient
H12	Shape factor $\delta_1/\delta_2$
M1	$2(1 + \eta) / (3 + 2\eta)$
M2	$(\eta^3 + 7\eta^2 + 12\eta + 4) / (\eta^2 (3 + 2\eta))$
M3	$\eta^2 (3 + 2\eta) / (\eta + 1)^2 (\eta + 2)^2$
r	Fillet radius
ST	Total channel length
$U_0$	Free stream inlet velocity
$U_e$	Free stream velocity
$U_{ex}$	X component of free stream velocity
$U_{ey}$	Y component of free stream velocity
$U_{eo}$	Free stream velocity along mid-channel streamline
$U_{exo}$	X component of free stream velocity along $\eta = 0$ .
$U_{eyo}$	Y component of free stream velocity along $\eta = 0$
X,Y	Coordinates of channel flow
$X_c$	Coordinate of intersection of bisector with corner boundary layer surface
$\delta_1$	Boundary layer displacement thickness
$\delta_2$	Boundary layer momentum thickness
$\delta_3$	Interference displacement thickness
$\delta_{2c}$	Corner boundary layer momentum thickness



## LIST OF SYMBOLS (CONCLUDED)

$\epsilon_0$	Endwall boundary layer thickness
$\eta$	Distance from stator endwall streamline
$\nu$	Kinematic viscosity
$\psi_1, \psi_2$	Streamfunctions
$\phi$	Measures inclination of $\sigma$ on Y axis
$\sigma$	Distance measured along channel streamline
$\Delta U_{ey}$	Change in tangential velocity over channel length
$\beta$	Parameter governing the inclination of isovels to the wall

## SECTION I

### INTRODUCTION

Based on an analysis presented in Reference 1, this report describes a procedure to calculate the parameters which determine the inception of separation at the intersection of a turbocompressor stator blade row airfoil and its adjacent platform or endwall. These parameters are then used to determine the geometry of a fillet which will prevent corner flow separation from occurring.

The report includes a computer program which was developed to calculate these parameters from a knowledge of blade row inlet and exit flow conditions and geometry.

An example of a typical calculation procedure of a corner fillet geometry is presented.

## SECTION II

### THEORY AND METHODS

#### 1. FLOW MODEL

Under consideration is the flow development in a compressor stator blade row in the vicinity of the corners formed by the blade suction and pressure sides and endwalls. The flow is assumed turbulent through the blade row.

The inviscid flow velocity in the channel may be calculated either from the method developed in Reference 2, assuming a circular arc blade (Figure 1), or directly obtained from a polynomial interpolation of data points (Figure 2).

Under the assumption of a circular arc blade, the free stream velocity is expressed as

$$U_e = \psi_1(\sigma) + \psi_2(\sigma) \eta,$$

where  $U_e$  is the velocity along a streamline,  $\eta$  is in the Y direction, and  $U_{ex}$  and  $U_{ey}$  are the X and Y components of  $U_e$  (Figure 3).

Furthermore,

$$\psi_2(\sigma) = -\pi (\Delta U_{ey}/2ST) \sin(\pi\sigma/ST),$$

where  $\Delta U_{ey} = U_{ey1} - U_{ey2}$  and  $U_{ey1}$  and  $U_{ey2}$  are tangential components of the velocity at the entrance and exit of the channel, respectively.  $ST$  is the length of the flow path in the blade row and  $\eta = 0$  defines the midchannel streamline so that the suction and pressure corners correspond to  $-\eta_s$  and  $+\eta_p$ , respectively.

With the subscript 0 designating mid-channel streamline conditions, we have:

$$U_{exo} = \text{constant} = U_{eo} \sin \phi,$$

where  $\phi = \text{arctg}(U_{ex}/U_{ey})$ .

Also,

$$U_{ey0} = \int_0^S \psi_2(\sigma) d\sigma + U_{ey01} = U_{ey01} - (\Delta U_{ey}/2) (1 - c\phi s (\pi\sigma/ST)).$$

Thus,

$$U_{eo} = (U_{exo}^2 + U_{ey0}^2)^{1/2} = \psi_1(\sigma)$$

and

$$U_e = U_{eo} - \frac{\pi\Delta U_{ey}}{2ST} \sin \frac{\pi\sigma}{ST} \eta. \quad (1)$$

The expression for the velocity gradient is, therefore,

$$\frac{\partial U_e}{\partial \sigma} = -\Delta U_{ey} \left[ 2\pi \sin\phi \sin\left(\frac{\pi\sigma}{ST}\right) \left\{ U_{ey1} + \Delta U_{ey} \left[ c\phi s \left(\frac{\pi\sigma}{ST}\right) - 1 \right] \right\} + \left(\frac{\pi}{ST}\right)^2 c\phi s \left(\frac{\pi\sigma}{ST}\right) \eta \right] \quad (2)$$

If interpolation of velocity data points is chosen, the expression for the free stream velocity and its first derivative in the channel is:

$$U_e = C1 + C2 X + C3 X^2 + C4 X^3 + C5 X^4 \quad (1')$$

and

$$\frac{dU_e}{dX} = C2 + 2C3 X + 3C3 X^2 + 4C5 X^3. \quad (2')$$

## 2. CALCULATION OF TWO-DIMENSIONAL BOUNDARY LAYER MOMENTUM THICKNESS

The two-dimensional flow boundary layer momentum thickness used in the evaluation of the shape factor H12 and, therefore, of  $\beta$  and  $\eta$ , is obtained from Truckenbrodt's quadrature (3). The expression for the two-dimensional boundary layer momentum thickness,  $\delta_2$ , is:

$$\delta_2(\sigma) = \left(\frac{U_e}{U_o}\right)^{-3} \left[ \text{ST}^{\frac{1}{n}} \left(\frac{C_f}{2}\right)^{\frac{n+1}{n}} \int_0^\sigma \left(\frac{U_e}{U_o}\right)^{\frac{3+2}{n}} d\sigma \right]^{\frac{n}{n+1}} \quad (3)$$

In this equation,  $n = 6$ .

The shape factor, H12, is obtained from Garner's equation (3):

$$\left(\frac{U_e \delta_2}{\nu}\right)^{\frac{1}{6}} \delta_2 \frac{dH12}{d\sigma} = -e^{5(H12-1.4)} \left( \left(\frac{U_e \delta_2}{\nu}\right)^{\frac{1}{6}} \frac{\delta_2}{U_e} \frac{dU_e}{d\sigma} + .0135 (H12-1.4) \right) \quad (4)$$

The boundary layer velocity profile power law exponent,  $n$ , is directly obtained from

$$H12 = \frac{(2+n)}{n}$$

With the assumption (1) that the ratio of the three-dimensional corner boundary layer extent  $\sigma$  to the two-dimensional boundary layer thickness  $\epsilon_0$  is approximately equal to 2,  $\beta$  is obtained from

$$2 = \left( \frac{\beta (n+1)(n+2)}{\left(\frac{2n\beta}{\beta+1} + 1\right) \left(\frac{2n\beta}{\beta+1} + 2\right)} \right)^{\left(\frac{1+\beta}{\beta-1}\right)} \quad (5)$$

The friction coefficient,  $C_f$ , is obtained from

$$C_f = 0.013 / (U_e \delta_2 / \nu)^{\frac{1}{6}}$$

## 3. CALCULATION OF CORNER FLOW PARAMETERS

The fact that secondary flows are always generated in the endwall boundary layer precludes using the two-dimensional boundary layer thickness directly derivable from Equation 3 as a basis for the calculation of corner flow parameters. Also, the presence of secondary flows causes the corner boundary layer to be markedly unsymmetrical. Nonetheless, by assuming, in the vicinity of the corner, the boundary layer thickness on the blade pressure and suction sides to be equal to that resulting on the endwall from the presence of secondary flows, the three-dimensional corner boundary layer becomes symmetrical. The calculation of the interference displacement thickness in the corner conducted according to the procedure developed in Reference 1, yields a value of this parameter which may be considered as an upper limit. According to Reference 1, this upper limit will lead to a conservative value of the fillet radius likely to prevent separation in the corner.

The qualitative nature of the results sought confers a particular interest on the method used by P. Suter to calculate the corner momentum thickness in Reference 2. Figure 3 shows that the development of the corner momentum thickness along the blade pressure and suction sides is virtually independent of the presence of secondary flows generated in the channel. This remark affords a significant simplification in the calculation of the interference displacement thickness since the parameters of the turbulent endwall boundary layer with secondary flow in the vicinity of the corner may be evaluated from a linear, first order differential equation,

$$\frac{\partial \delta_{2c}}{\partial \sigma} M1 + \frac{\partial U_e}{U_e \partial \sigma} \delta_{2c} (2 + M2) = C_f, \quad (6)$$

instead of a system of two non-linear partial differential equations, Reference 2

$$\begin{aligned} \frac{\partial}{\partial X} (U_{ex}^2 \delta_2) + \frac{\partial}{\partial Y} \left[ U_{ex} U_{ey} (\delta_2 + Dh) \right] + H12 \delta_2 \left( U_{ex} \frac{\partial U_{ex}}{\partial X} + U_{ey} \frac{\partial U_{ex}}{\partial Y} \right) \\ - B_{11} h U_{ey} \frac{\partial U_{ex}}{\partial Y} = \frac{C_f}{2} U_{ex} U_e \end{aligned} \quad (7)$$

$$\frac{\partial}{\partial X} \left[ U_{ex} U_{ey} (\delta_2 - B_{21} h) \right] + \frac{\partial}{\partial Y} \left[ U_{ey}^2 (\delta_2 + Ah - \frac{Eh^2}{\Delta_2}) \right] + \delta_2 H_{12} (U_{ex} \frac{\partial U_{ey}}{\partial X} + U_{ey} \frac{\partial U_{ex}}{\partial Y}) - B_{11} h U_{ey} \frac{\partial U_{ey}}{\partial Y} = \frac{C_f}{2} U_e U_{ey} \left[ 1 + \frac{m}{(2m+1)(m+1)} \frac{h}{\delta_2} \right]. \quad (7)$$

In solving Equation 6, the parameters M1 and M2, as well as the friction coefficient  $C_f$  are considered to vary along the streamline.

The three-dimensional corner boundary layer parameter  $\delta_{2c}$  obtained from Equation 6 may be defined as the average corner momentum thickness at a particular location along the corner. The definitions and hypotheses used in the derivation of Equation 6 by P. Suter directly yield the result that  $X_c$ , the coordinate of the intersection of the corner bisector with the corner boundary layer surface, may be expressed as

$$X_c = \delta_{2c} / M3.$$

The thickness and the momentum thickness of the endwall boundary layer with secondary flow, in the corner, can, in turn (From Reference 1) be written:

$$\epsilon_0 = 2 \frac{-1}{1+\beta} X_c$$

and

$$\delta_2 = \epsilon_0 (H_{12} - 1) / (H_{12} (H_{12} + 1)). \quad (8)$$

According to Reference 1, the interference displacement thickness,  $\delta_3$ , is:

$$\delta_3 = \left\{ X_c^2 - \frac{2n^2 \beta X_c}{(n+1)[\beta(2n+1)+1]} \frac{[\beta(2n+1)+1]}{n\beta} \epsilon_0^{\frac{-1}{n}} \delta^{\frac{-1}{n\beta}} + \frac{2 \beta \epsilon_0 \delta^{\frac{1}{\beta}}}{(\beta-1)(n+1)} \left( \delta^{\frac{\beta-1}{\beta}} - X_c^{\frac{\beta-1}{\beta}} \right) + \frac{\epsilon_0^2}{2n+1} - \frac{2\epsilon_0 \delta}{n+1} \right\}^{\frac{1}{2}} \quad (9)$$

#### 4. DETERMINATION OF FILLET RADIUS LIKELY TO PREVENT CORNER FLOW SEPARATION

As explained in Reference 1, the maximum value of  $\delta_3$  along the suction or pressure corner is used directly to determine the fillet radius likely to prevent corner flow separation. For this purpose, Figure 5 reproduced from Reference 1 is used. The procedure may be described:

(a) For the Reynolds number applicable to the channel flow under consideration, obtain directly from Figure 4 a "safe" value of the maximum corner interference displacement thickness. For  $Re = 10^6$ , for instance,  $\delta_3/L$  could be chosen between .007 and .01.

(b) From the maximum value of  $\delta_3$  calculated from Equation 9 and the "safe" value of  $\delta_3$  chosen in (a), estimate the percent decrease in  $\delta_3$  which will prevent corner flow separation.

(c) Use the desired percent decrease obtained in (b) to estimate from Figure 5 the desirable fillet radius to be provided in the corner from the channel entrance to the location of maximum  $\delta_3$ .

#### 5. REMARKS CONCERNING THE CALCULATION OF $H_{12}$ , $\beta$ , AND EU

The average value of the Euler number,

$$AVEU = \frac{\int_0^{XMN} EU dx}{\int_0^{XMN} dx},$$

where

$$EU = \frac{-L}{U_0^2} \frac{dP}{dx},$$

is calculated along the mid-channel streamline, XMN, the upper limit of the integral, is the value of X at which the minimum value of the mid-channel free stream velocity occurs.



On an airfoil or in a constant pressure gradient diffuser, entire separation of the flow takes place when  $AVEU = -.25$ . This is not necessarily so in the general case of an axial-flow compressor stator channel where values of  $AVEU < -.25$  have been obtained without flow separation. It would be expected that values of  $AVEU < -.25$  could occur far downstream, in the neighborhood of  $X = XMN$ , and that calculation of corner flow parameters could be continued from this point on, assuming no flow separation. Likewise, the validity of the results displayed in Figure 4 would hold and the limit value of  $-.25$  could be used in estimating the fillet radius from Figure 5.

$H12$  and, therefore,  $n$  are calculated for the main flow along the pressure and suction corners. The preceding comments on the limit values of  $AVEU$  apply to  $H12$  since it is also a separation parameter. Boundary layer separation occurs on an airfoil when  $1.8 < H12 < 2.2$ . For values of  $H12 = 1.74$  and above, Equation 5 yields values of  $\beta = 1$  and  $\beta < 1$  when  $\delta/\epsilon_0 = 2$ . Since  $\beta$  cannot be  $< 1$ , Reference 1,  $\delta/\epsilon_0$  must be allowed to assume values  $> 2$ . Figure 6 shows the variations of  $H12$  and  $\delta/\epsilon_0$  along the pressure corner for the example chosen in this report.

It must be noted that the variation of  $\delta/\epsilon_0$  is to be interpreted as an average value of this parameter between the entrance plane and the value of  $X$  at which the maximum value of  $H12$  occurs. In Figure 6, the peak value of  $\delta/\epsilon_0$  is, in fact, the minimum value which  $\delta/\epsilon_0$  may assume for the associated value of  $H12$  (Reference 1). Consideration of the experimental values obtained for  $\beta$ ,  $\delta/\epsilon_0$ , and  $n$  in the case of a mildly adverse pressure gradient (Reference 1) makes the assumption that  $\beta$  is very near 1 for the strongly adverse pressure gradients prevailing in compressor stator channels quite reasonable.

## SECTION III

## NUMERICAL EXAMPLE

The numerical data used in this example was obtained from Technical Report AFAPL-TR-76-92 and generated with a single stage axial-flow compressor operating at 100% speed near peak efficiency. The data describes average values of entrance and exit flow parameters of the stator channel and its physical dimensions. In addition, the main flow velocity profile along the suction and pressure side corners was scaled from data calculated by the three-dimensional computer program "NANCY 1.0" of AiResearch Manufacturing Company of Arizona.

Listed below are the average values of the velocity at entrance and exit planes and the physical dimensions of the channel.

Channel width	2.54 cm.	1 in.
Channel length	6.35 cm.	2.5 in.
Reynolds number		$10^6$
Meridional Velocity	204.52 m/s	671. ft/sec
Initial Tangential Velocity	253.18 m/s	831. ft/sec
Exit Tangential Velocity	9.4 m/s	30.82 ft/sec
Initial Momentum Thickness	.0038 cm.	0.0015 in.
Initial H12		1.47

The results of corner flow boundary layer parameters calculation as performed by the computer program listed in the Appendix are presented in Figures 7 through 17. From these results, the evaluation of the corner fillet radius is easily performed. For the pressure corner, for instance, the maximum value of  $\delta_{3/L}$ , which occurs at  $S/L = .836$  in., is .037 (Figure 16). It is seen that, from Figure 4, for  $RE = 10^6$ , a safe value of  $\delta_{3/L}$  may be taken as 0.007, so that the percent decrease in  $\delta_{3/L}$  sought is 81.2%. Figure 5 is then used, in conjunction with the average Euler

number, in this case equal to  $-.246$ , to find the value of the fillet radius, which is  $0.22$  in. Similarly, for the suction side, Figure 17, indicates that the maximum value of  $\delta_{3/L}$  is  $.04083$ , occurring at the trailing edge. The desired decrease in  $\delta_{3/L}$  sought is  $82.86\%$ , which, in conjunction with an average Euler number of  $-.246$  yields a fillet radius of  $0.28$  in.

#### 1. REMARKS

The discussion presented in the chapter CONCLUSION of Reference 1 applies directly to the contents of this report. This is particularly true for the considerations governing the fillet radius profile along the corner.

## APPENDIX

## NUMERICAL METHODS (PROGRAM FILLET)

This program involves the solution of three linear, first order partial differential equations. These equations (3, 4, and 6) are integrated using a fourth order Runge-Kutta method. The parameter  $\beta$  of the power law velocity is obtained from Equation 5, using a polynomial approximation.

## 1. PROGRAM STRUCTURE

This program consists of a main program and four subroutines.

## (1) Main Program:

(a) Calculates the free stream velocity and velocity gradient along a streamline.

(b) Calculates simultaneously the friction coefficient, endwall momentum displacement thickness form coefficient  $H_{12}$ , and corner momentum displacement thickness.

## (2) Subroutines:

(a) Subroutines "POLYNO" and "LINEQ" use a polynomial approximation to calculate the free stream velocity and the velocity gradient along the suction and pressure corners.

(b) Subroutine "INTICK" calculates the corner interference displacement thickness.

(c) Subroutine "FILLET" calculates the optimum fillet radius along the suction and pressure corners.

(d) Subroutine "AVEREUL" calculates the coordinates of WSX minimum used in the calculation of the Euler number.

## 2. PROGRAM AND SUBPROGRAM DESCRIPTIONS

## Main Program

<u>Calculation</u>	<u>Equation</u>	<u>First Card</u>
Determine free stream velocity	1	103, 115
Determine free stream velocity gradient	2	111, 118
Calculate $\int_{\sigma}^0 (U_e/U_o)^{3.333} d\sigma$ using Simpson's numerical integration method		149
Determine 2-D boundary layer thickness using Truckenbrodt's quadrature	3	175
Calculate shape factor H12	4	198
Calculate corner boundary layer momentum thickness	6	216
Calculate turbulent 3-D endwall momentum thickness	8	220

## Subroutine INTICK

<u>Calculation</u>	<u>Equation</u>	<u>First Card</u>
Determine interference displacement thickness	9	5

## Subroutines POLYNO and LINEQ

Calculation

Calculate M + 1 coefficients of  
polynomial of order n used in the  
calculation of WSX and DWSX.

## Subroutine FILLET

Calculation

Calculate optimum corner fillet  
radius.

## Subroutine AVEREUL

Calculation

Calculate minimum value of WSX and X  
at which this minimum occurs.

## 3. FORTRAN NOMENCLATURE

<u>Variable</u>	<u>Description</u>
ALPHA	Supplementary angle of dihedral
AVEU	Average value of Euler number
BETA	Parameter governing the inclination of isovels to the wall
C, CM	Velocity polynomial coefficients
CBL	Coordinate of intersection of bisector with corner boundary layer surface
CFX	Skin friction coefficient
CFX1	CFX at $X + \text{DELX}/2$
CFX2	CFX at $X + \text{DELX}$
CONSW	X component of free stream velocity along mid-channel streamline
DEL	Extent of three-dimensional corner flow
DELPRT	$\delta/\epsilon_0$
DELX	Incremental step along X
DEL2X	Boundary layer momentum thickness from Truckenbrodt's quadrature
DEL2XS	Endwall boundary layer momentum thickness from Suter's hypothesis
DEL2X1	DEL2X at $X + \text{DELX}/2$
DEL2X2	DEL2X at $X + \text{DELX}$
DEL3	Corner interference displacement thickness
DEL3MAX	Maximum value of DEL3

<u>Variable</u>	<u>Description</u>
DEL3X	Corner boundary layer momentum thickness
DEWY	Channel entrance and exit tangential velocity difference
DWSX, DWSXM	Free stream velocity gradient
EPSO	Endwall boundary layer thickness
ETNA	Distance from stator mid-channel endwall streamline
EULE	Euler number
EUM	Average value of Euler number
EXN	Inverse exponent in power law for primary velocity profile
H12	Form factor
NDA	Corner interference displacement area
PERCNT	Percent decrease in DEL3MAX required to prevent corner flow separation
RAFIL	Value of corner fillet radius required to obtain percent decrease in DEL3MAX
SIBX	Sine of angle measuring direction of free stream velocity W·R·T· Y axis
SIGM	X values for VEL
ST	Length of channel measured along mid streamline
VEL	Free stream velocity input data
WSX	Free stream velocity
WSXO	Total velocity at channel entrance
WSXØ	WSX initial value
WY1	Tangential velocity at channel entrance
X	Distance along streamline
YMIT, YMIN	Coordinates of WSX minimum

## 4. INPUT DATA

Three input data formats are used: alphanumeric, integer, and real. Each record, or card, contains only one type of data, and normal FORTRAN convention indicates which are the integer quantities. The alphanumeric format is used for the title cards and consists of eighty characters starting in the first column. The integers are entered in fields of four characters with up to twenty numbers per card. No decimal point may be used and the number should be right justified within the allocated field. The real numbers are entered in fields of twelve, with up to six numbers per card and a decimal point should be entered to ensure correct interpretation of the data. The first field on each card begins in column 1.

In the following chart, one line corresponds to one card, except where it has been necessary to use two lines to complete the description of one card.

CARD 1: TITLE

CARD 2: X $\emptyset$ , XS, ALPHA, WSX $\emptyset$ , WSX0, DEL2X1

CARD 3: DEL2X2, DEL2 $\emptyset$ , H12, ST, WSFF

CARD 4: N $\emptyset$ P, N $\emptyset$ D, N, M, M1, L

CARD 5: WY1, DEWY, C $\emptyset$ NSW, ETNA, DEL3X

CARD 6: VEL(K), SIGM(K)} This card occurs M times

CARD 7: VELM(K), SIGM(K)} This card occurs M1 times

## 5. DEFINITION OF INPUT DATA ITEMS

TITLE	Alphanumeric title for job. Up to eighty characters may be used starting in column 1.
X $\emptyset$	Initial value of left hand boundary used in subroutine "AVREUL".
XS	Initial value of independent variable "X" along a given streamline.



ALPHA	Supplementary angle of dihedral (Reference 1).
WSXØ	Initial value of WSX.
WSX0	Total velocity at channel entrance.
DEL2X1	DEL2X at $X + DELX/2$ .
DEL2X2	DEL2X at $X + DELX$
DEL2Ø	Initial endwall boundary layer momentum thickness from Suter's hypothesis (see note).
H12	Form factor.
ST	Length of channel measured along mid streamline.
WSFF	Channel exit free stream velocity.
NØP	If NØP = 0, Suter's equation 1 is used to calculate the free stream velocities along the mid-channel and suction or pressure corner streamlines, using the following decimal variables: WY1, DEWY, CØNSW, ETNA.  If NØP ≠ 0, a polynomial, $l'$ , is used to calculate the non-dimensional free stream velocities along the mid-channel and suction or pressure corner streamlines from the experimental data entered on input data cards 6 and 7.
NØD	If NØD = 0, all computed data is listed. If NØD ≠ 0, only DEL3MAX, EUM, PERCNT, and RAFIL are listed.
N	Integer variable giving iteration interval.
M	Number of velocity data points along corner streamline.
M1	Number of velocity data points along mid-channel streamline.
L	Degree + 1 of polynomial used in the interpolation of velocity data points. Maximum value of L is 10.

WY1	Tangential velocity at channel entrance (non-dimensional).
DEWY	Channel entrance and exit tangential velocity difference (non-dimensional).
CØNSW	X component of free stream velocity along mid-channel streamline (non-dimensional).
ETNA	Distance from stator mid-channel endwall streamline (dimensionless).
DEL3X	Initial corner boundary layer momentum thickness (see note).
VEL(K)	Corner free stream velocity data input. The maximum value of K is 100.
SIGM(K)	Distance along streamline.
VELM(K)	Mid-channel free stream velocity.

NOTE: The initial value of the two-dimensional boundary layer momentum thickness is obtained from Falkner's equation (reference pp. 632):

$$\frac{C_f}{2} = \frac{.0065}{(WSXO * DEL2Ø/v)^{1/6}}$$

with the friction coefficient,  $C_f$ , obtained from reference p.p. 600, for the Reynolds number of interest.

In the example given here,  $C_f = .0045$ ,  $Re = 10^6$ , so that  $DEL2Ø = .00145$ .

The initial value of DEL3X is directly obtained from the initial value of DEL2Ø, using P. Suter's assumption that, at the channel entrance, the ratio  $DEL3X/DEL2Ø = 1.55$ .

## 6. OUTPUT DATA

The printed output consists of two sections. First, the input data is completely listed. Following this are printed the results computed by the program. If  $N\emptyset D = 0$ , the bulk of the calculated data is printed out.

If  $N\emptyset D \neq 0$ , only selected items from the computed data are printed out.

Description of calculated output data:

### I. $N\emptyset D = 0$ .

Are printed in the following order:

The coefficients of the polynomial used in the interpolation of WSX data.

The calculated values of WSX at data points, using curve fit polynomial.

The coefficients of the polynomial used in the interpolation of WSXM from data.

The calculated values of WSXM at data points, using curve fit polynomial.

The minimum value of WSXM along the mid-channel streamline.

The calculated boundary layer parameters: X, WSX, AVEU, H12, DEL2X, DEL3X, DEL2XS, EPS $\emptyset$ , EXN, BETA, DEL3.

The required fillet radius along the corner.

The percent drop in DEL3MAX to prevent separation.

The average value of the Euler number along the mid-channel streamline.

The maximum non-dimensional interference displacement thickness.

### II. $N\emptyset D \neq 0$

Only the last four items of the preceding list ( $N\emptyset D = 0$ ) are printed.

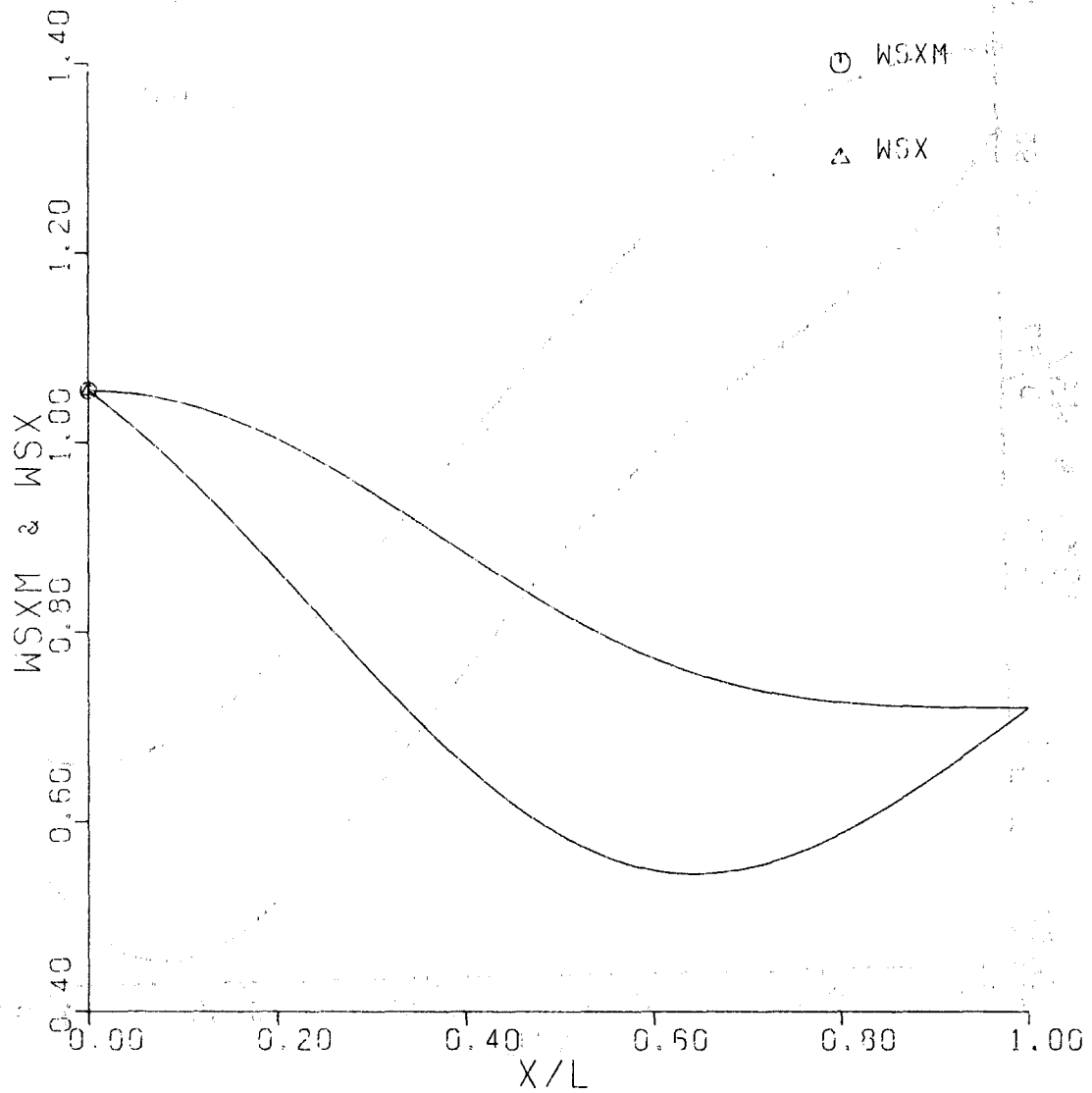


Figure 1. Non-Dimensional Velocity Along Mid-Channel and Pressure Corner Streamlines Assuming Circular Arc Blade

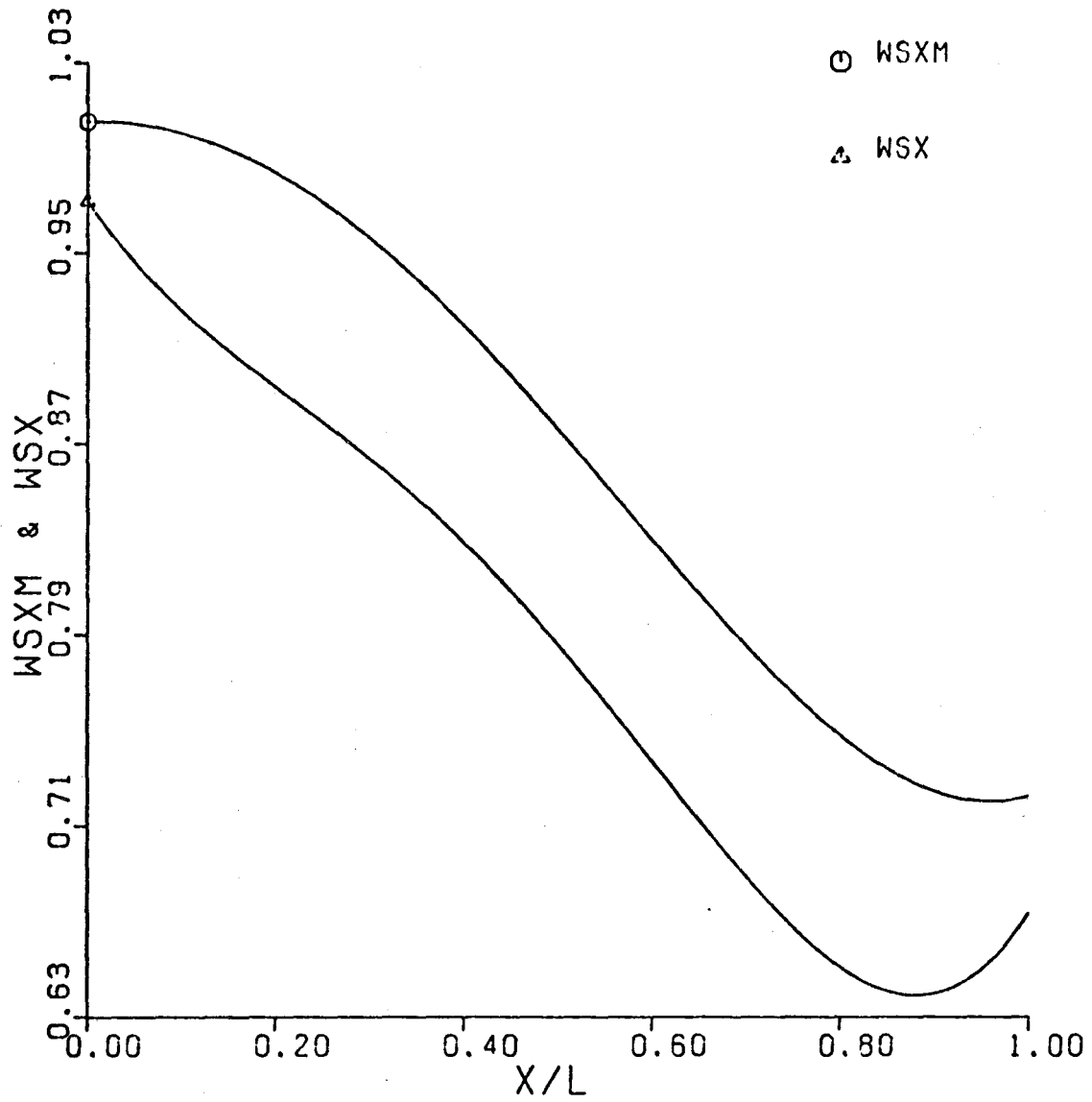


Figure 2. Non-Dimensional Velocity Along Mid-Channel and Pressure Corner Streamlines From Polynomial Interpolation of Data Points

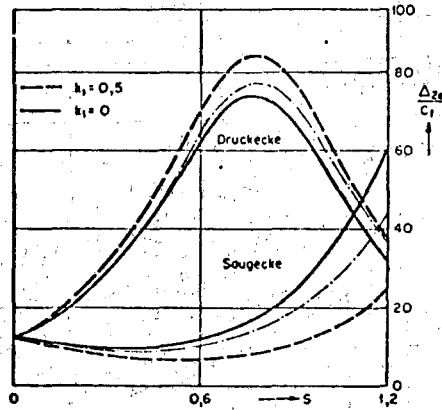


Figure 3. Influence of Endwall Boundary Layer Secondary Flow on the Development of Corner Boundary Layer

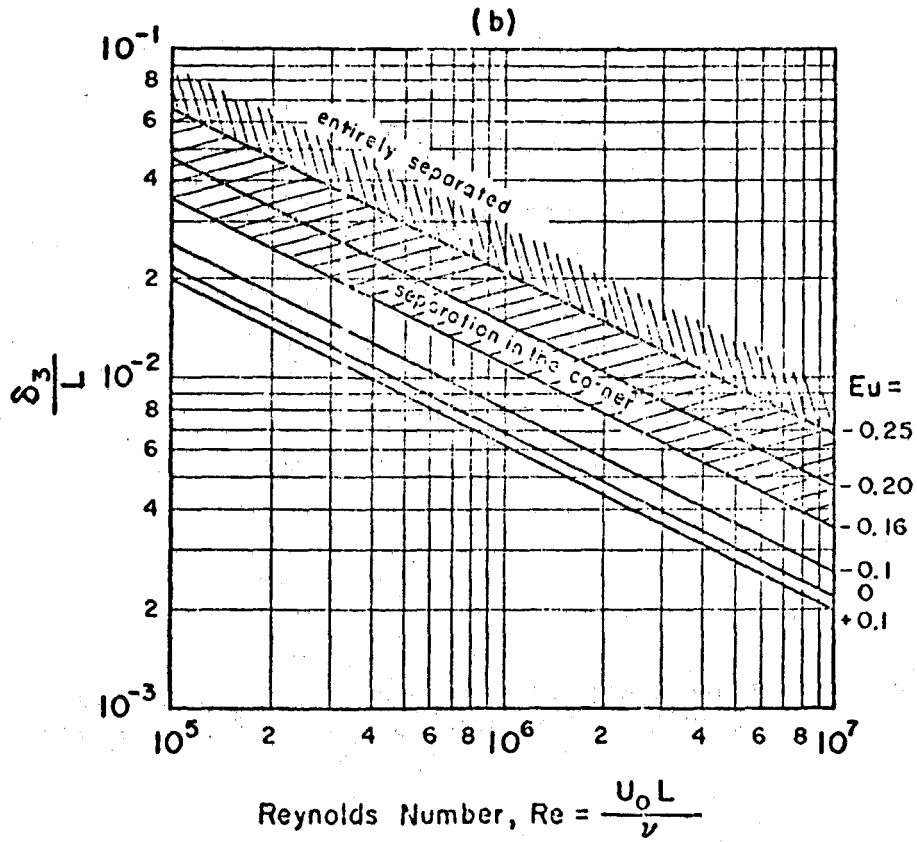


Figure 4. Interference Displacement Thickness of Turbulent Boundary Layer in Convergent or Divergent Flow Along a Corner From (3)

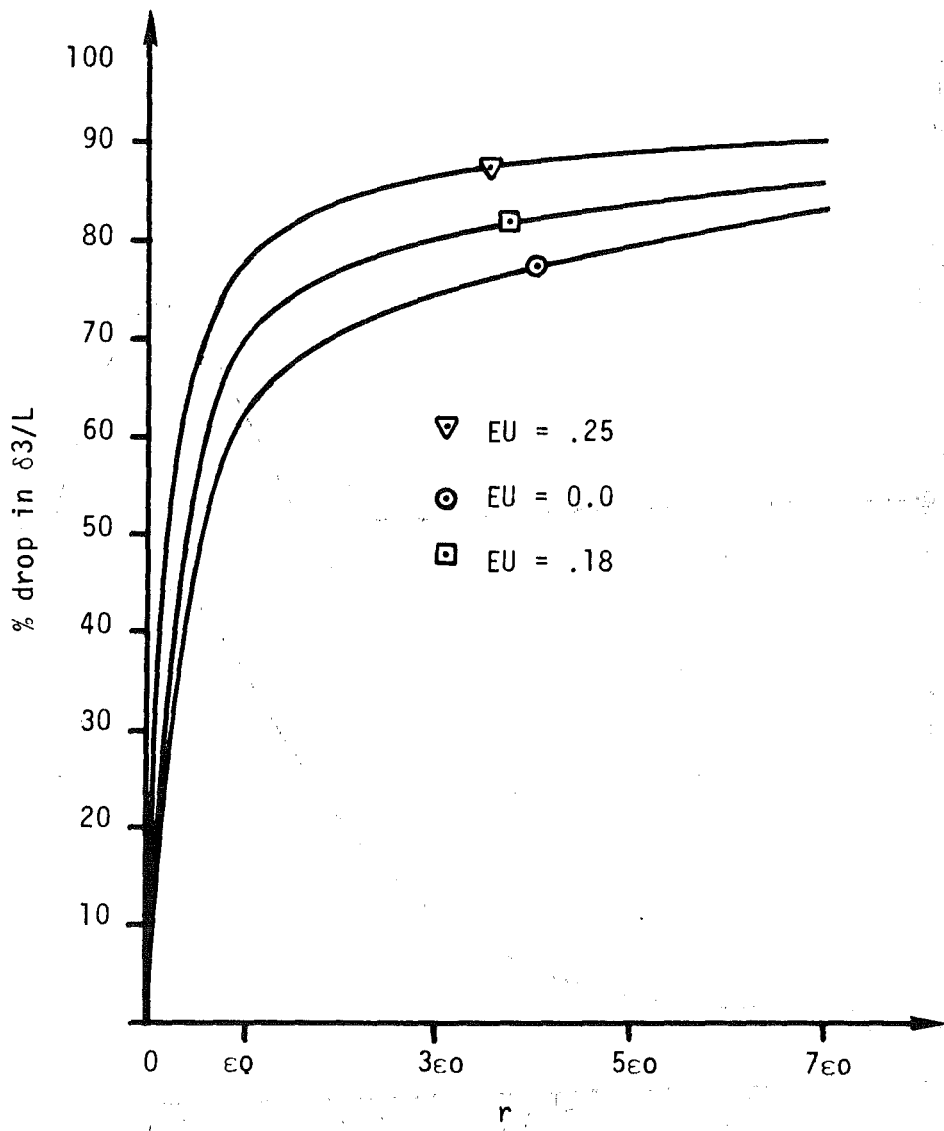


Figure 5. Percentage Drop in Interference Displacement Thickness vs Fillet Radius



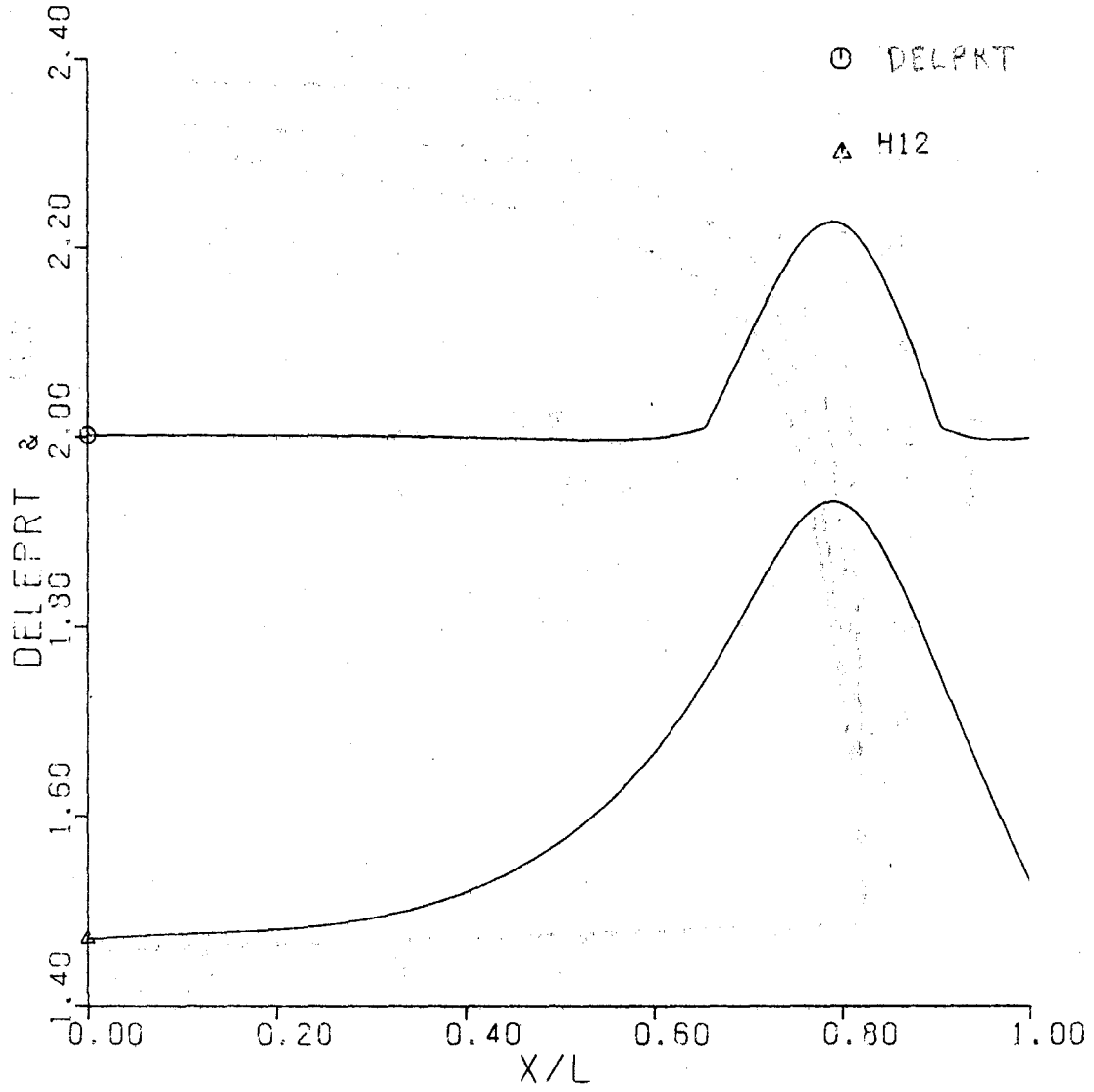


Figure 6. Variation of H12 and  $\delta/\epsilon$  Along the Pressure Corner

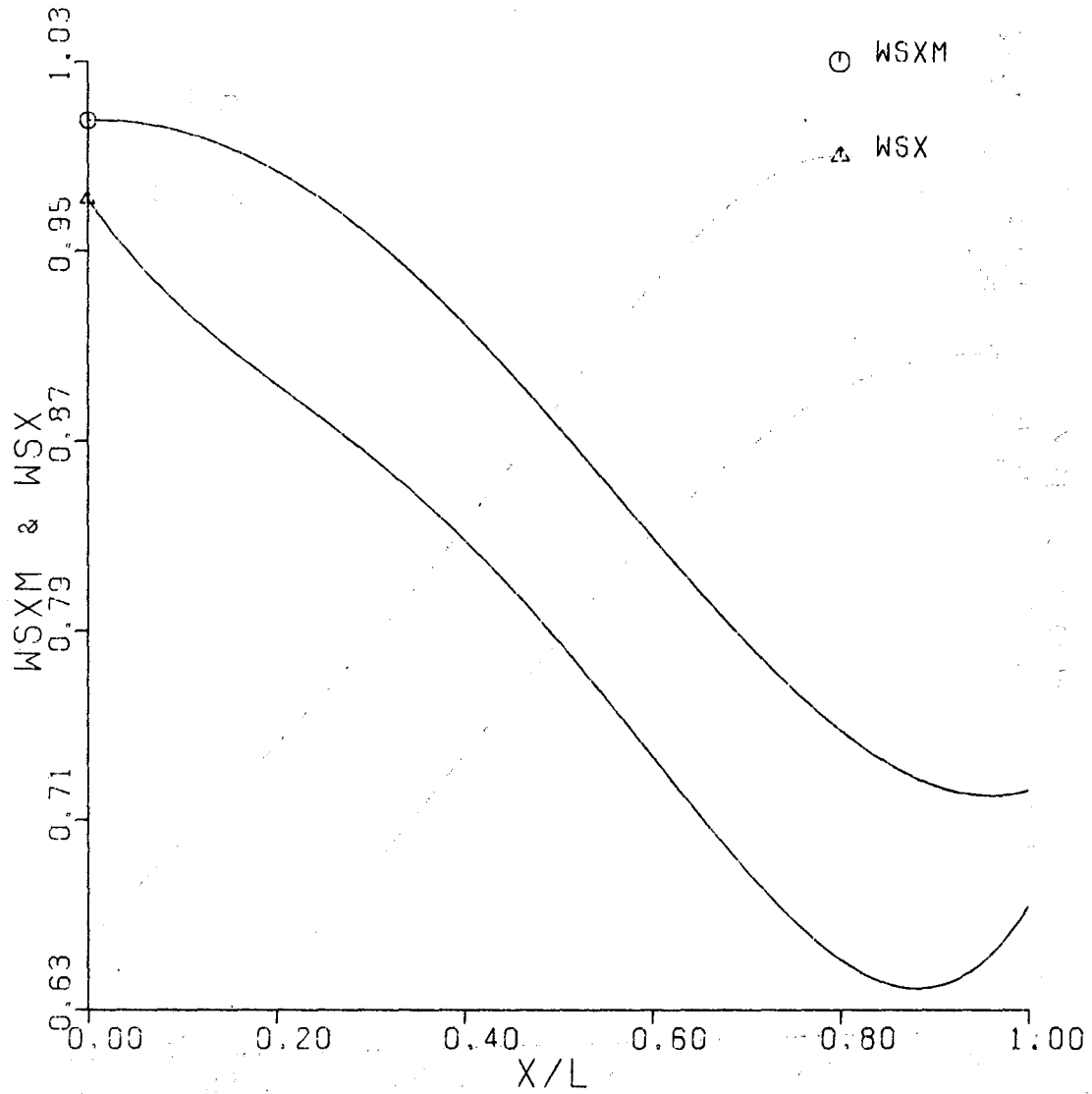


Figure 7. Non-Dimensional Velocity Profile Along Mid-Channel Streamline (WSXM) and Pressure Corner (WSX)

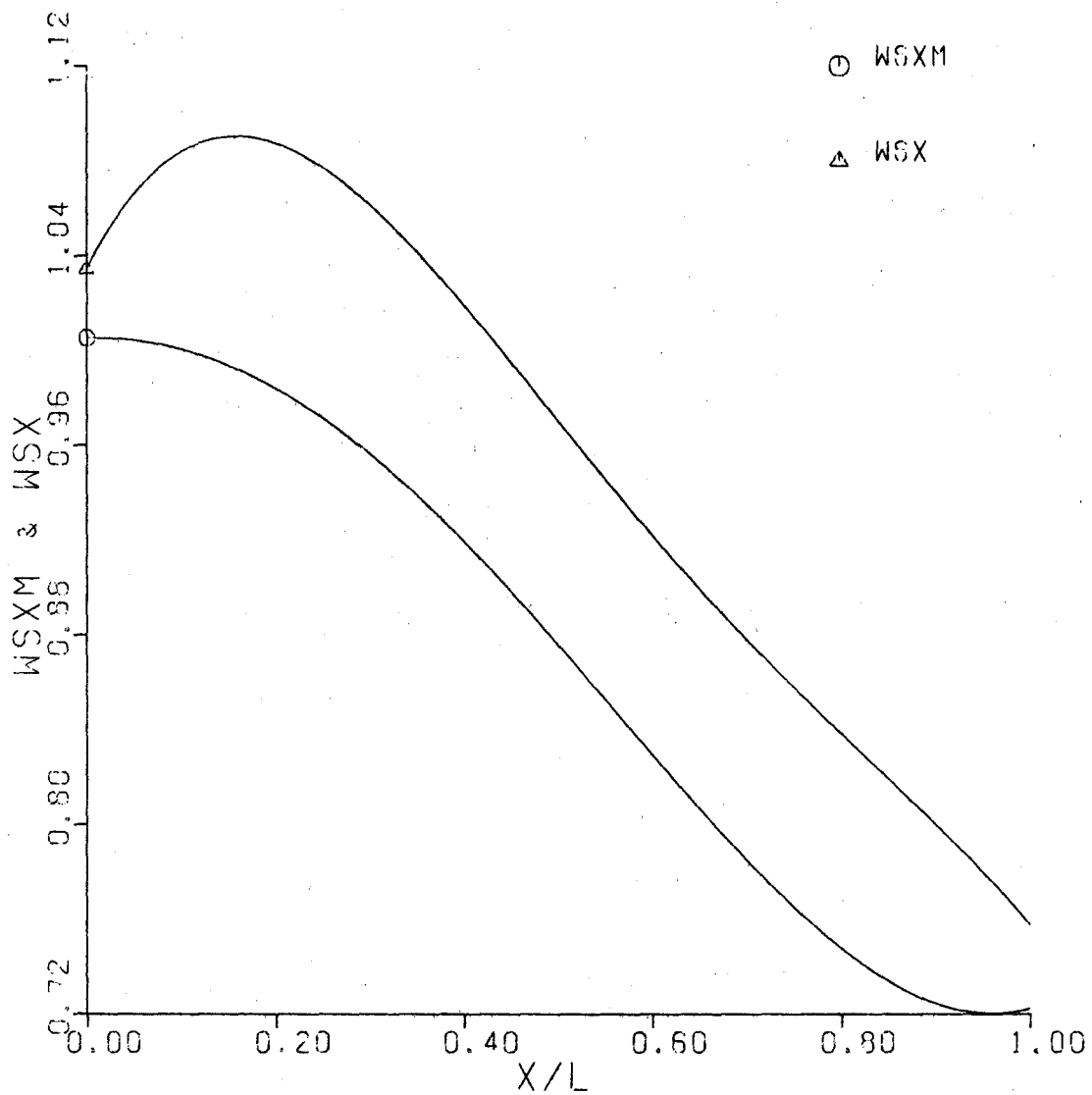


Figure 8. Non-Dimensional Velocity Profile Along Mid-Channel (WSXM) and Suction Corner (WSX) Streamlines

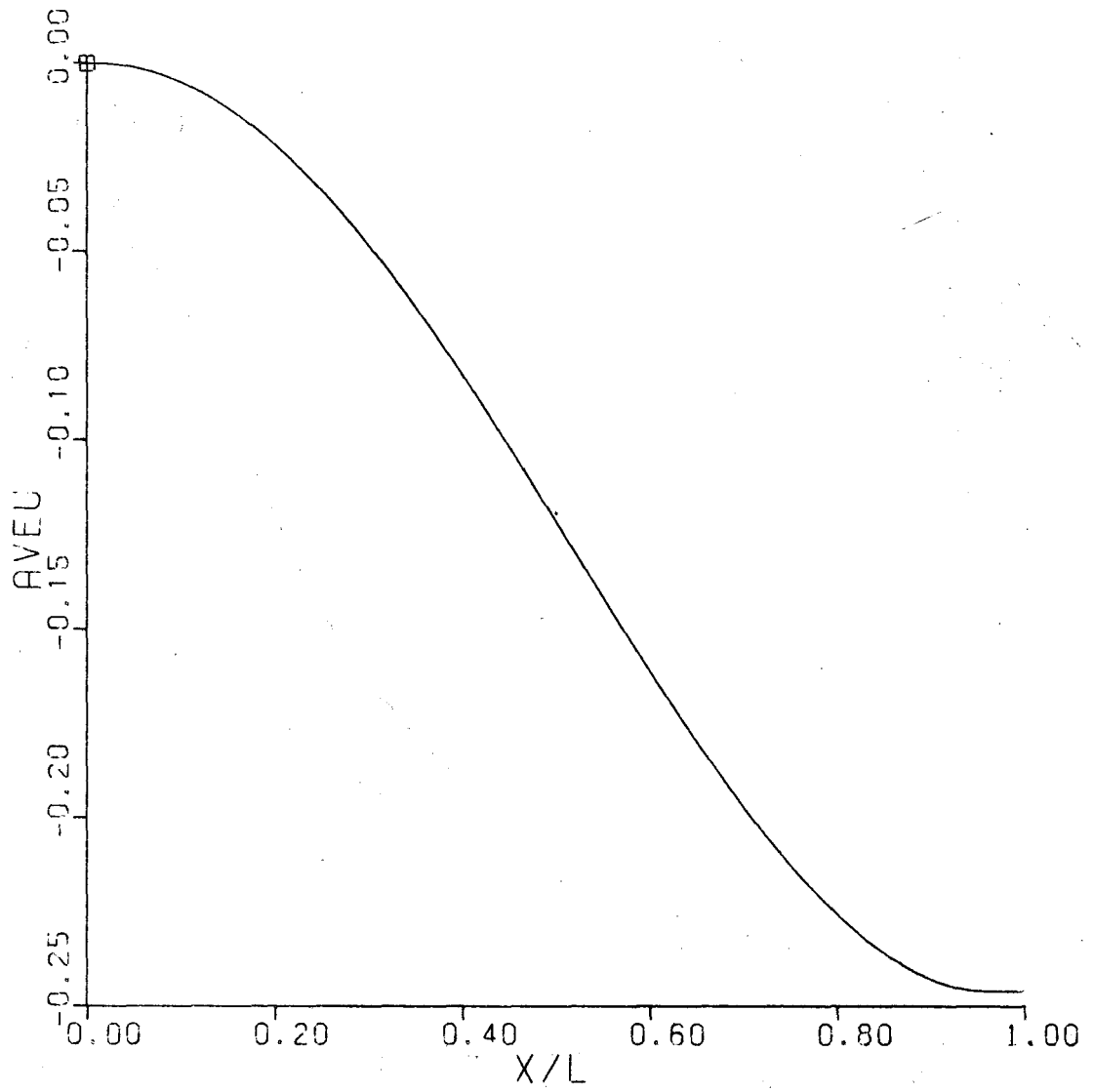


Figure 9. Average Euler Number Calculated Along Mid-Channel Streamline

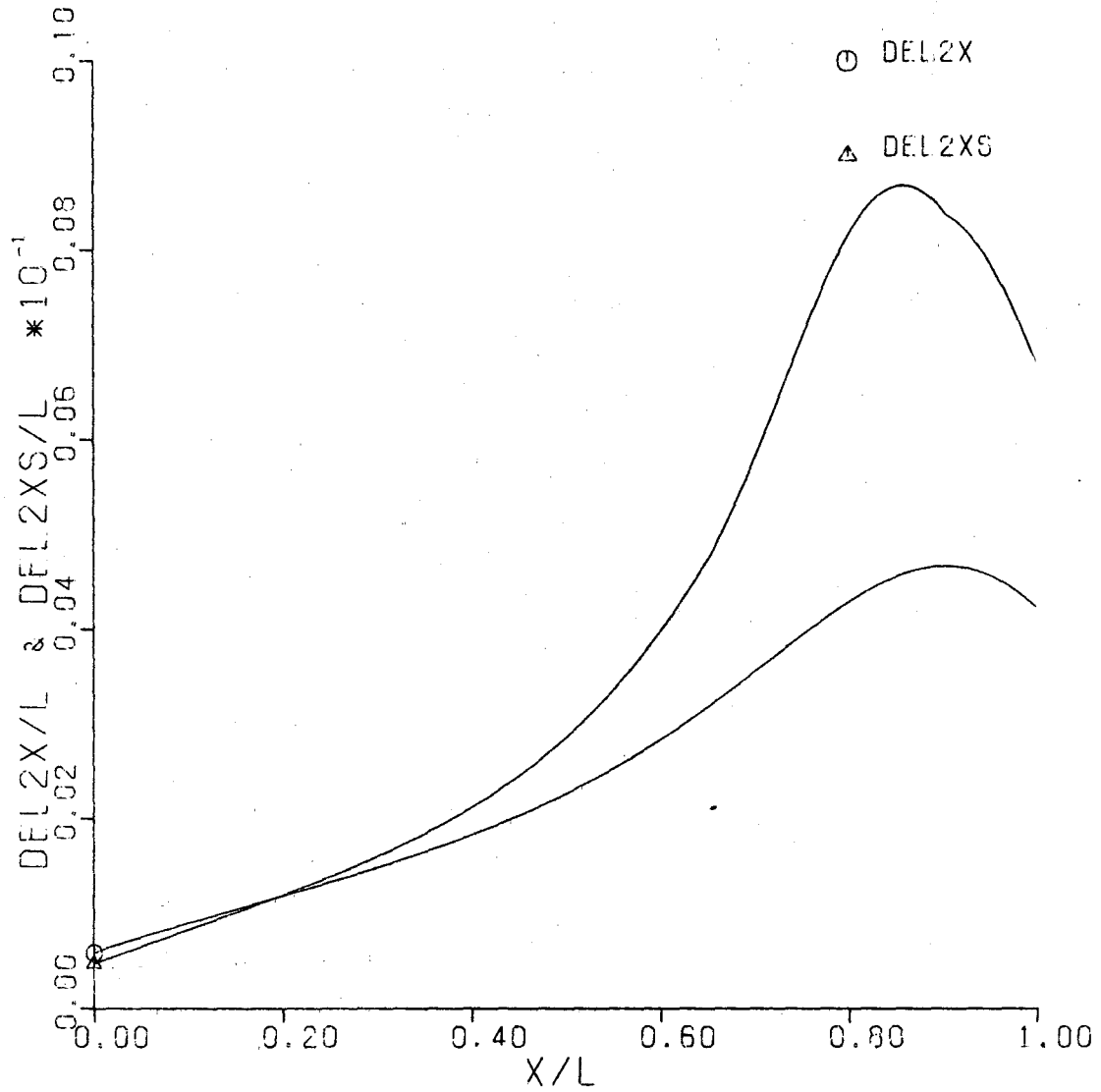


Figure 10. Two-Dimensional (DEL2X) and Three-Dimensional (DEL2XS) Boundary Layer Momentum Thickness Along Pressure Corner

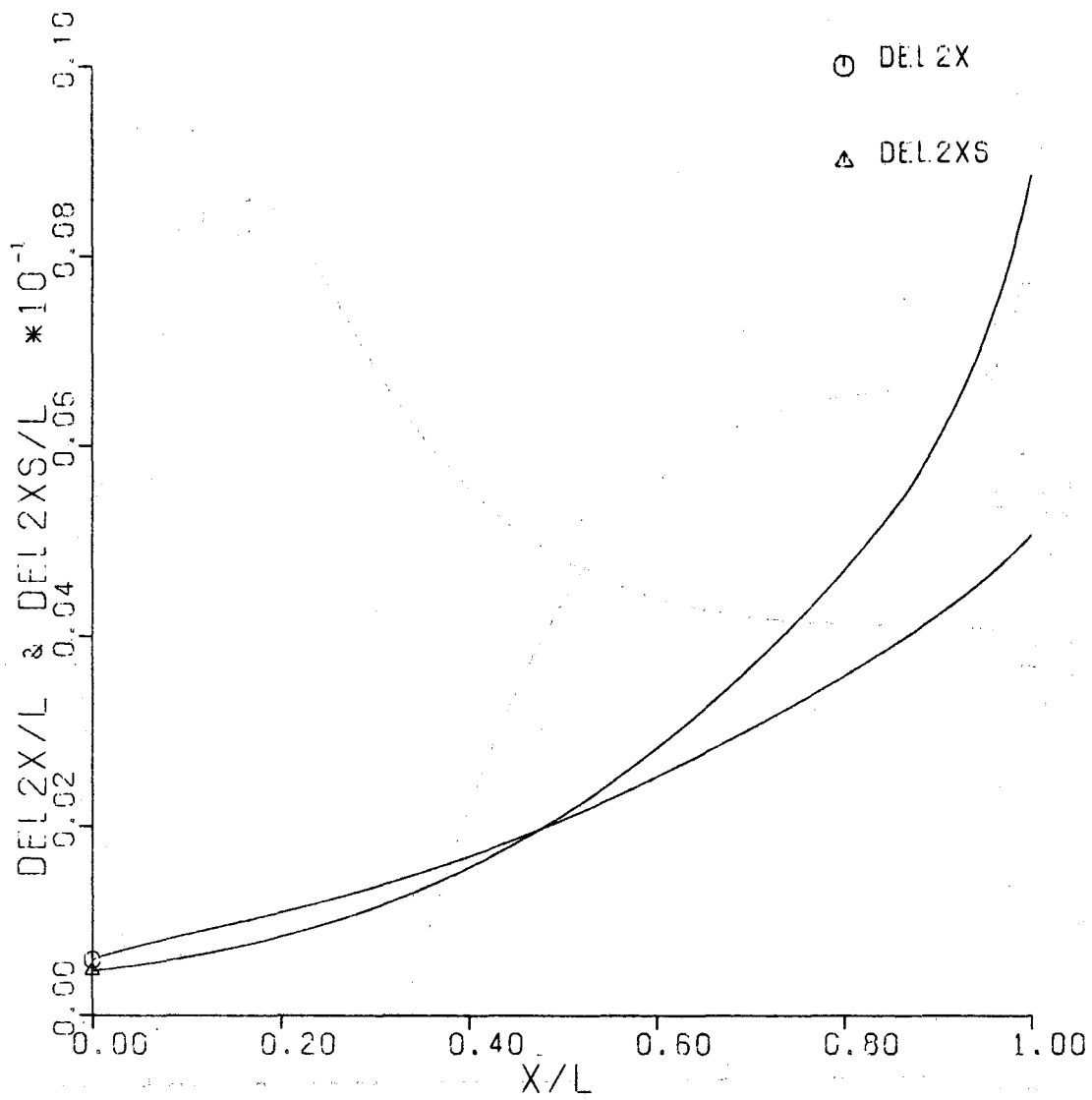


Figure 11. Two-Dimensional (DEL2X) and Three-Dimensional (DEL2XS) Boundary Layer Momentum Thickness Along Suction Corner

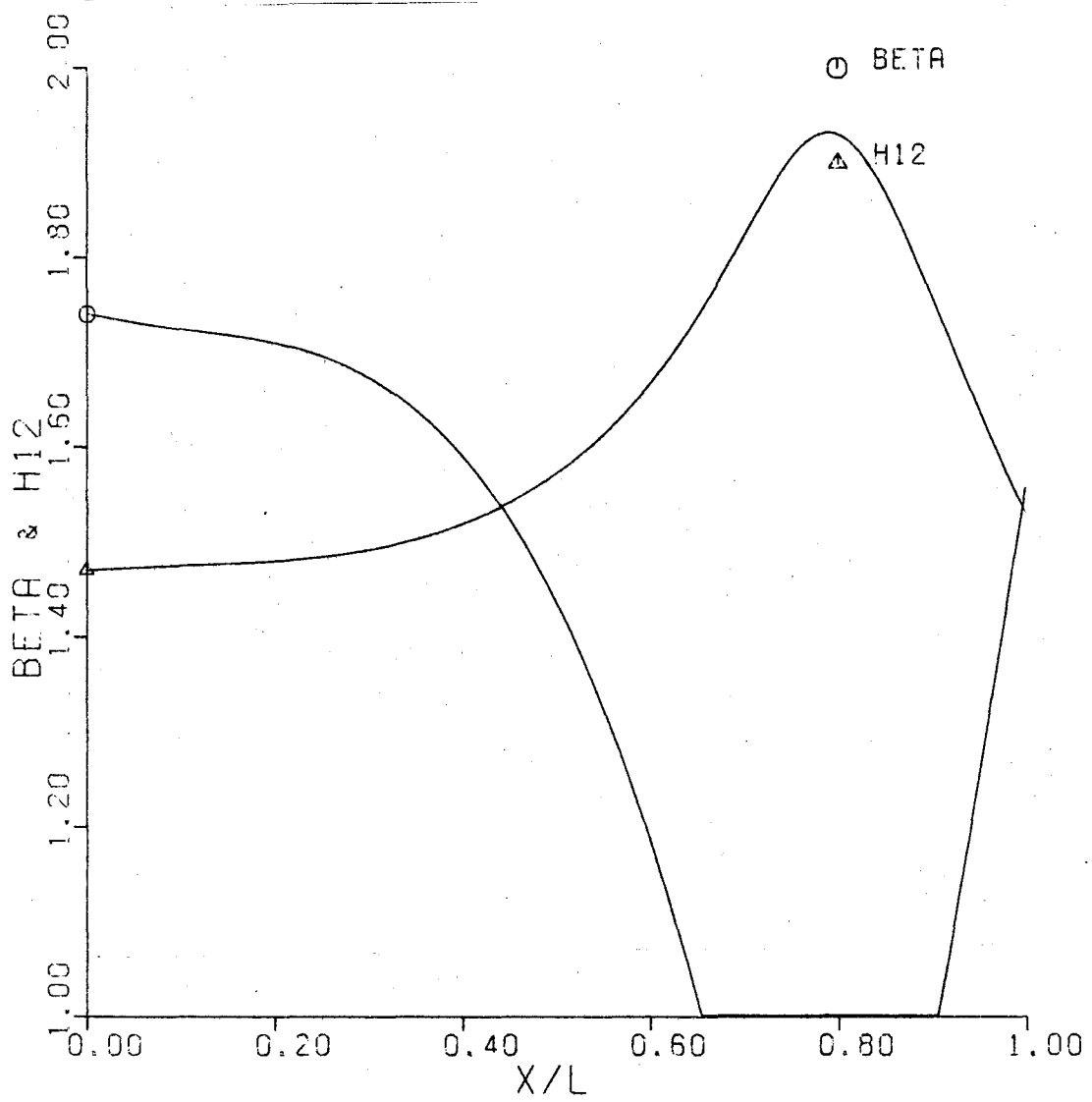


Figure 12. Variation of  $\beta$  and H12 Along Pressure Corner

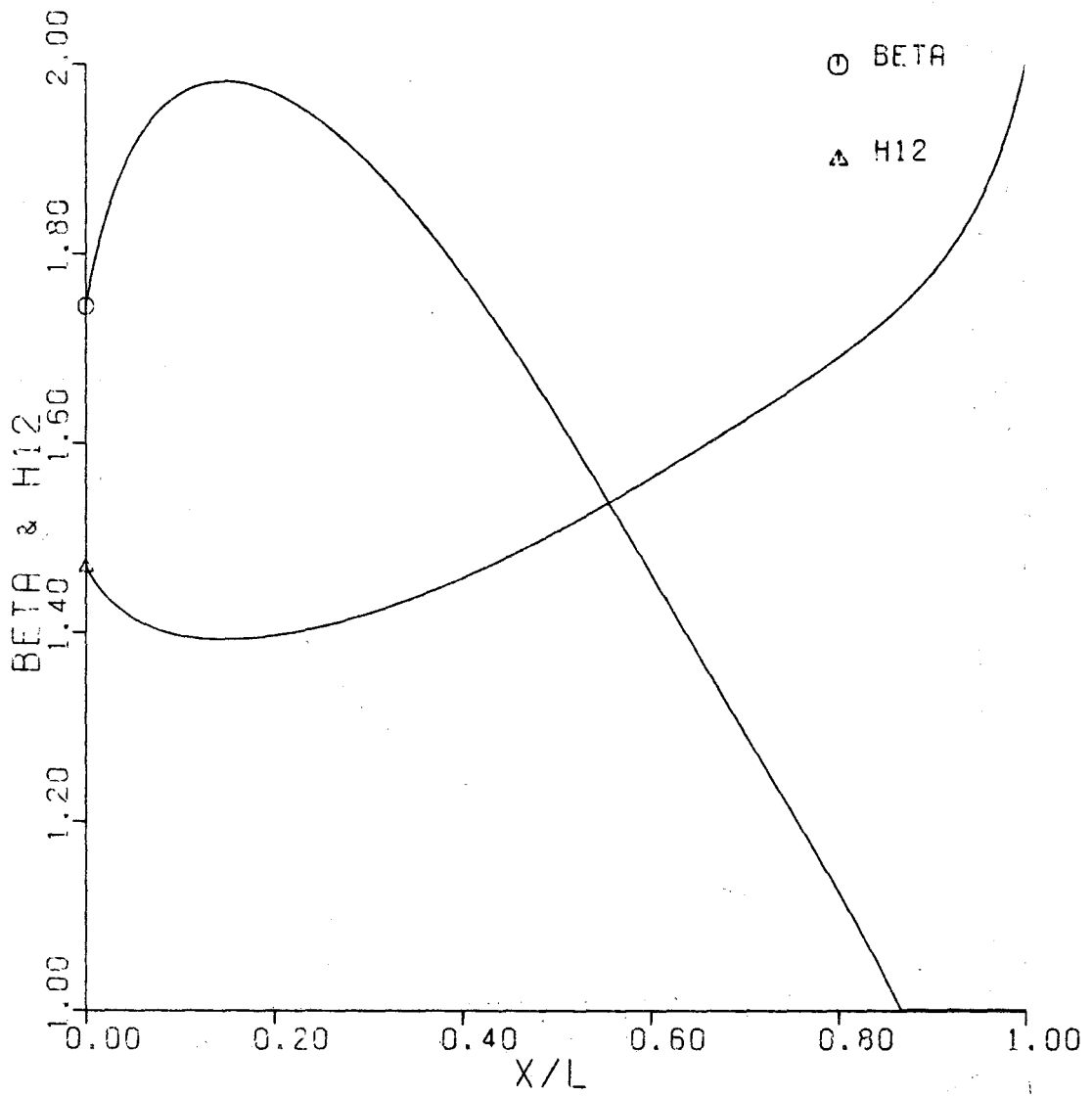


Figure 13. Variation of  $\beta$  and H12 Along Suction Corner



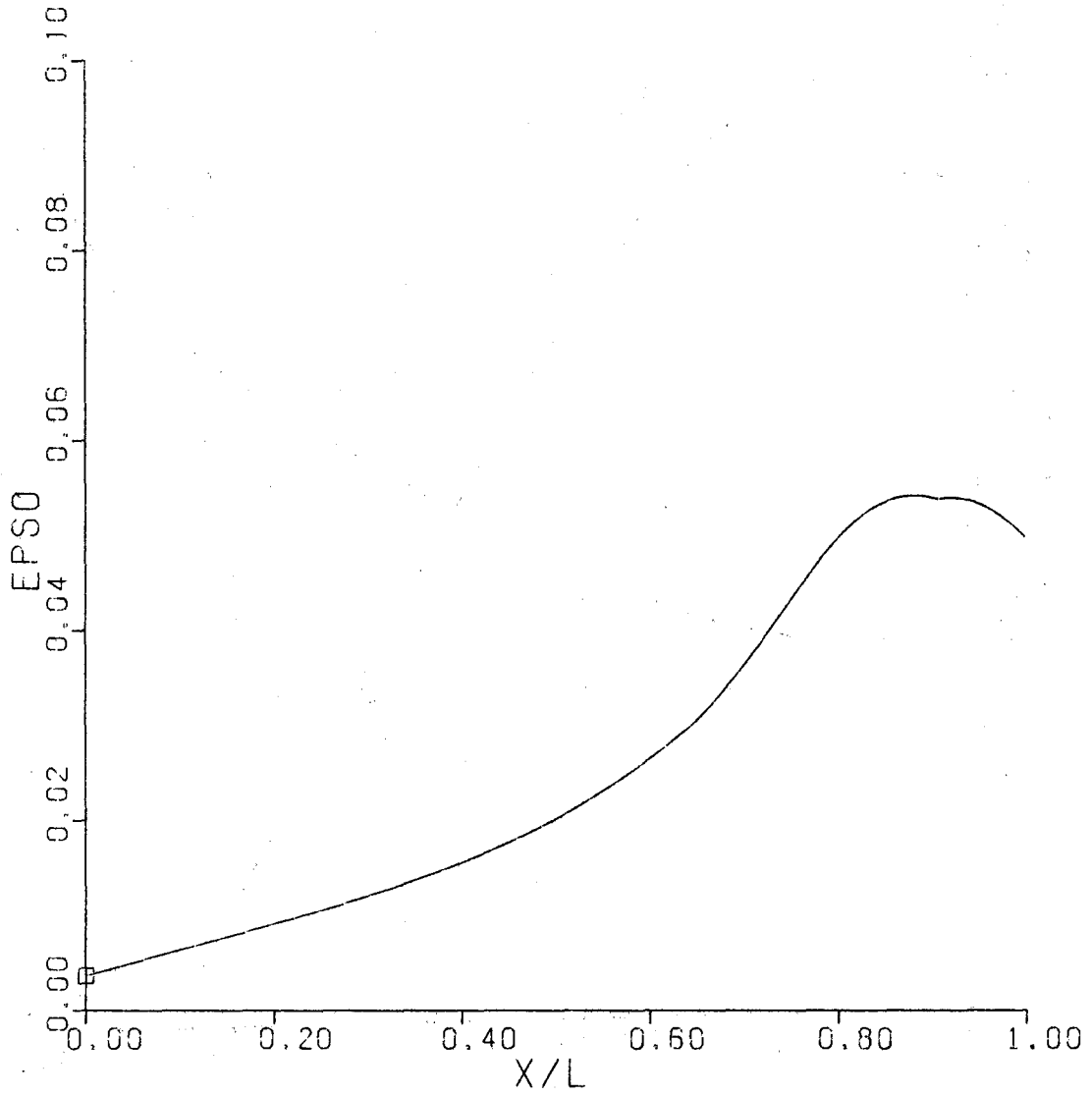


Figure 14. Variation of Endwall Boundary Layer Thickness Along Pressure Corner

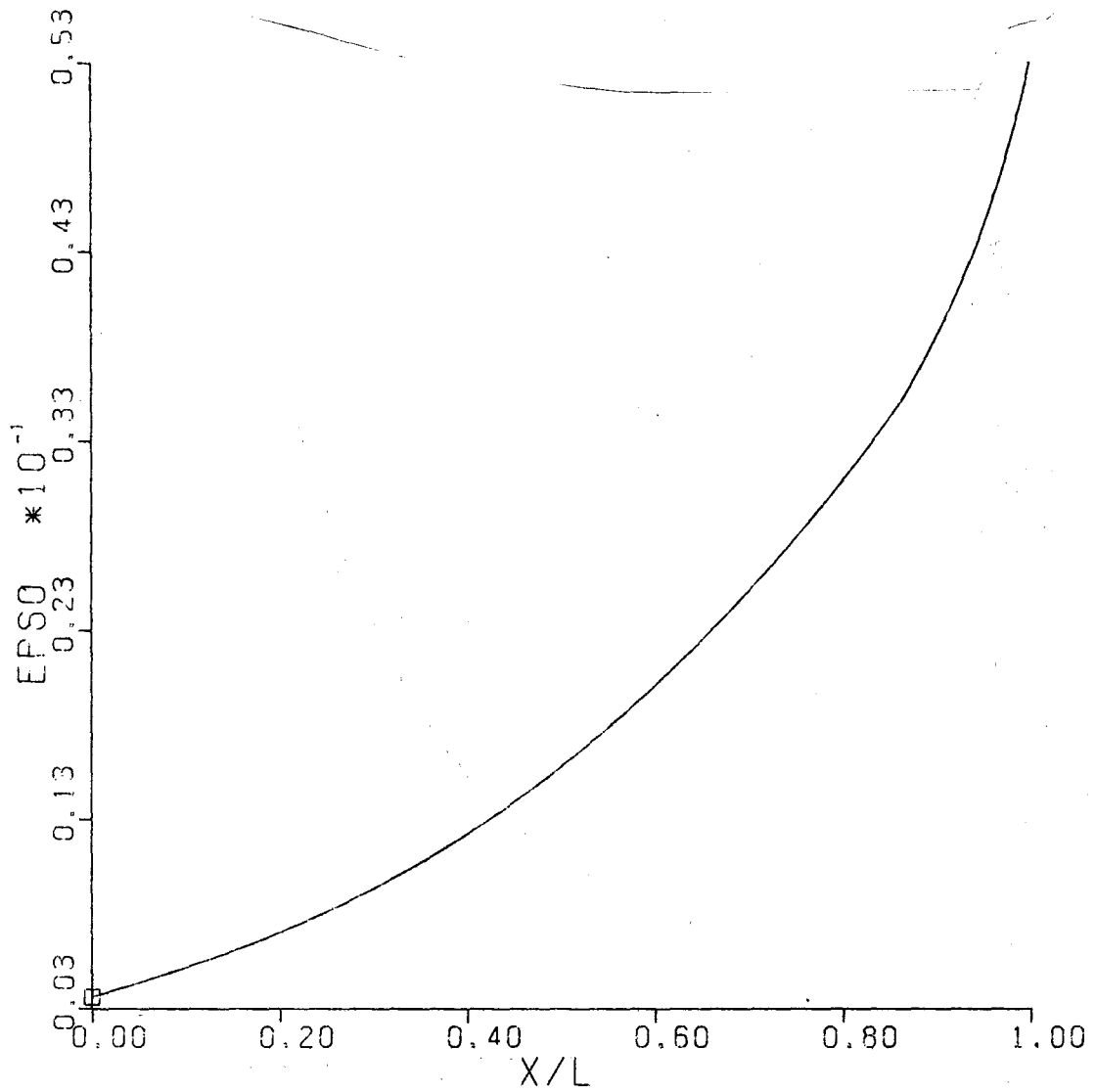


Figure 15. Variation of Endwall Boundary Layer Thickness  $\epsilon_0$  Along Suction Corner

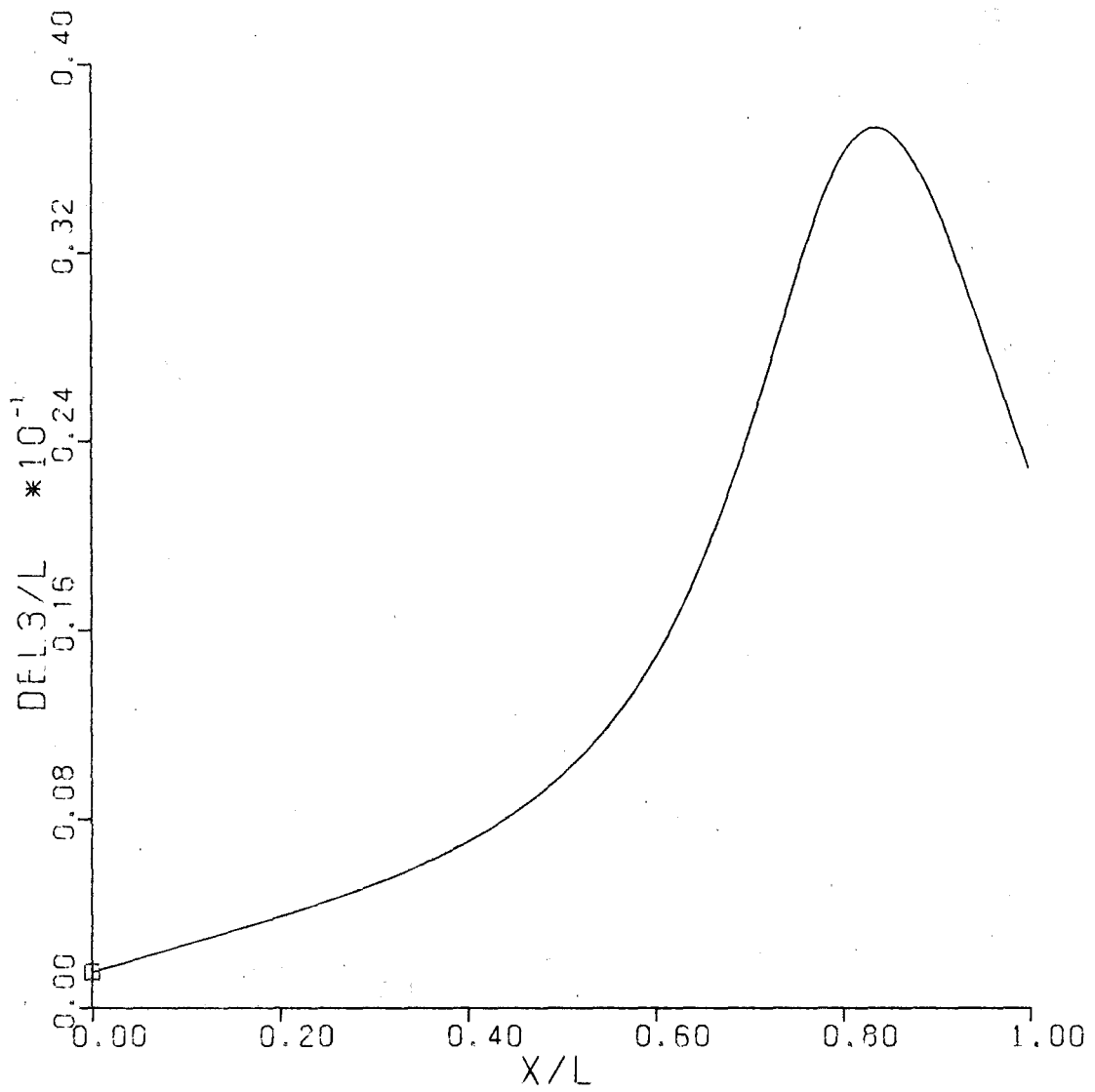


Figure 16. Variation of Corner Interference Displacement Thickness in Pressure Corner.

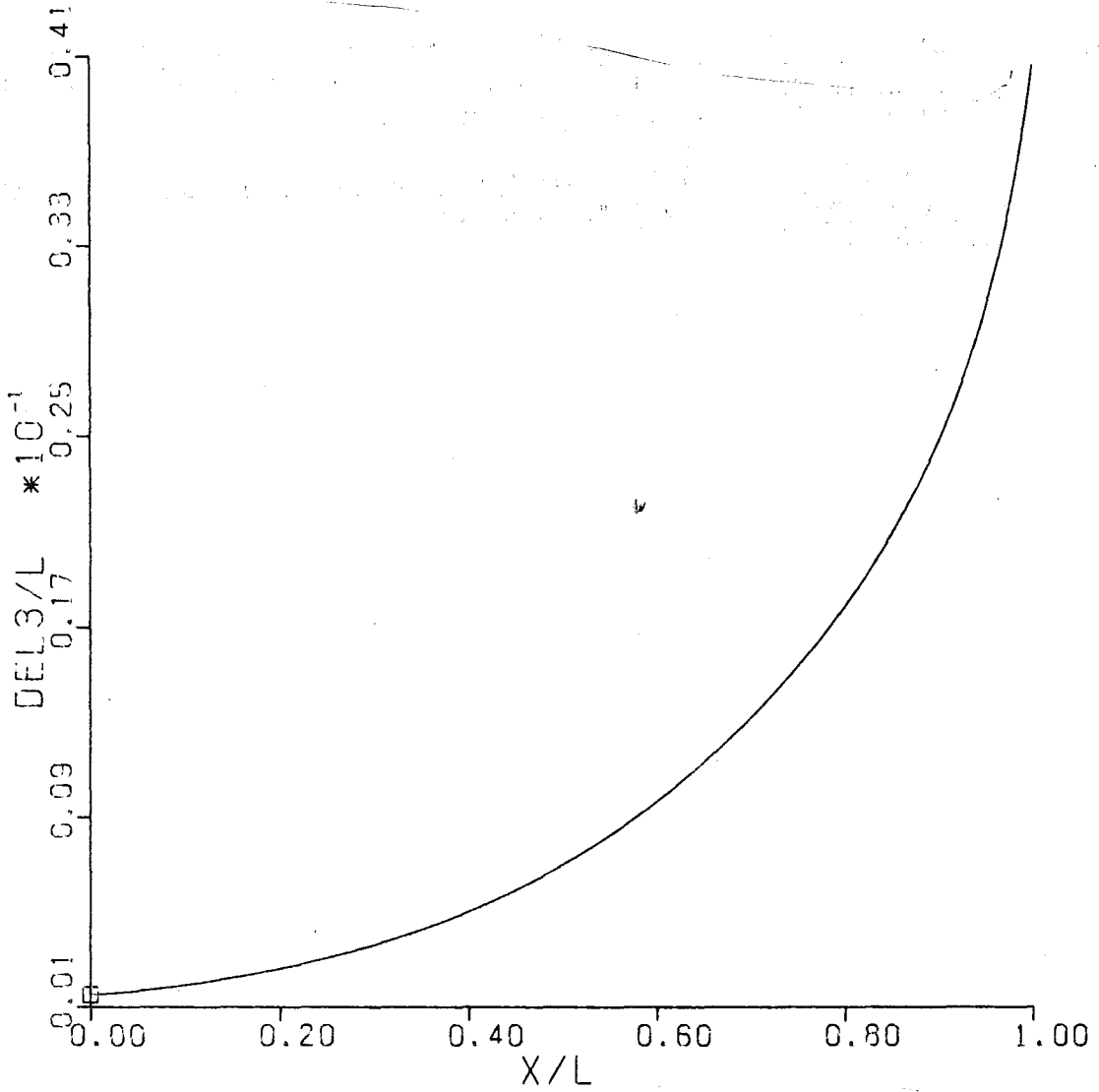


Figure 17. Variation of Corner Interference Displacement Thickness in Suction Corner

REFERENCES

1. L. L. Debruge, "The Aerodynamic Significance of Fillet Geometry in Turbocompressor Blade Rows," Journal of Engineering for Power, Vol. 102, October 1980.
2. P. Suter, Theoretical Untersuchung Uber die Seitenwandgrenzschichten in Axial Verdichtern, Mitteilungen aus dem Institut fur Thermische Turbomaschinen, Zurich, Switzerland, 1960, pp. 93-101.
3. H. Schlichting, The Incompressible Turbulent Boundary Layer with Pressure Gradient, Boundary Layer Theory, 6th Edition, McGraw-Hill, NY, 1968, pp. 627-643.